Journal of Power Sources 203 (2012) 206–210

Contents lists available at SciVerse ScienceDirect

Journal of Power Sources

journal homepage: www.elsevier.com/locate/jpowsour

Short communication

A study on $AgCuO_2$ as ultra fast charging cathode material for alkaline secondary battery

Junqing Pan[a,*], Yanbin Qiu[a], Yanzhi Sun[b,*], Zihao Wang[a]

[a] State Key Laboratory of Chemical Resource Engineering, Beijing University of Chemical Technology, Beijing 100029, China
[b] National Fundamental Research Laboratory of New Hazardous Chemicals Assessment and Accident Analysis, Beijing University of Chemical Technology, Beijing 100029, China

ARTICLE INFO

Article history:
Received 1 July 2011
Received in revised form 31 October 2011
Accepted 15 November 2011
Available online 23 November 2011

Keywords:
Silver cuprate
High charge/discharge rate
Alkaline secondary battery

ABSTRACT

$AgCuO_2$ as ultra fast charging cathode material for alkaline secondary batteries is reported in the present paper. The structural characterization shows that the $AgCuO_2$ material is composed of many one-dimension linear crystals arranged in a certain sequence. The experimental results show that the $AgCuO_2$ electrodes have good electrochemical characteristics at ultra fast charging-discharging speed from 5000 mA g^{-1} to 50,000 mA g^{-1}. The super high speed ability of charge/discharge makes the charge time of the electrode shorter than 29 s. Cyclic voltammetric (CV) and galvanostatic charge–discharge tests reveal that the charge/discharge process is not the single electron transfer for Cu(III) but the fast dual electron transfer for Ag(II) and Cu(III). The characteristics of high cycling capacity and fast charging for $AgCuO_2$ not only increase the specific capacity of batteries considerably but also make it possible to charge the future electric cars instantaneously as fast as refueling the fuel vehicles.

1. Introduction

With the development of digital products and electric automobiles, people have paid more and more attention to the high speed charge/discharge characteristic of batteries [1–3]. Kang and Ceder reported that the recently developed lithium ion batteries can be charged in less than two minutes for electric cars or 30 s for cell phones [4]. However, the aqueous electrolyte batteries, for example, Ni-metal hydride based ones, have serious drawbacks at high charge/discharge current [5]. Although the AgO cathode makes the charge time shorter than 2 min 53 s, its charge speed still needs to be improved [6].

The Ag–Cu dual metal oxides ($AgCuO_2$ and Ag_2CuO_3) were discovered in 1999, and there were a few reports about their discharge performance and the discharge mechanism in alkaline electrolyte [7–11]. Theoretically, the reduction of $AgCuO_2$ during discharge process needs as many as 4 electrons since it contains trivalent copper and univalent silver. Consequently, $AgCuO_2$ might have much higher capacity than MnO_2 and $Ni(OH)_2$ of single electron discharge[12]. However, the charge for Cu(II) to Cu(III) is considered to be very difficult because of the strong oxidizability of Cu(III), leading to a view point which deems that the realization of charge process for $AgCuO_2$ consisting of Ag(I) and Cu(III) is also hard. Therefore, its potential rechargeabilty and fast charging ability have not been reported until now.

In this paper, we report $AgCuO_2$ as ultra fast charge material for alkaline secondary batteries. The $AgCuO_2$ electrode has cycling specific capacity of 352 mAh g^{-1} at high charge/discharge rate of 50,000 mA g^{-1}. Consequently, the charge time is shortened to 29 s, making it possible to charge the electric cars instantaneously as fast as refueling the fuel vehicles. The electrochemical reaction mechanism of the $AgCuO_2$ electrode is also explored in the present paper.

2. Experimental

2.1. The preparation of $AgCuO_2$ samples

0.02 mol $AgCuO_2$ and 0.02 mol $Cu(NO_3)_2$ were dissolved in 0.1 mol L^{-1} HNO_3, and then the solution was added to 50 mL mixture solution consisting of NaClO (4.6 mol L^{-1}) and NaOH (7.5 mol L^{-1}) drop by drop with controlling speed at 3.0 mL min^{-1}, and then the suspension was aged for 60 min under 800 rpm stirring speed and 10 °C constant temperature before centrifugation. The product was then washed to present neutral by deionized water. After drying under vacuum at 323 K for 3 h, a black powder of $AgCuO_2$ sample was obtained.

2.2. The structural characterization of nano-structured $AgCuO_2$

The phase structures of $AgCuO_2$ samples were characterized by X-ray powder diffraction (XRD) using a Rigaku D/Max 2500

* Corresponding authors. Tel.: +86 10 64449332; fax: +86 10 64449332.
E-mail addresses: jqpan@mail.buct.edu.cn (J. Pan), sunyanzhi@sohu.com (Y. Sun).

0378-7753/$ – see front matter Crown Copyright © 2011 Published by Elsevier B.V. All rights reserved.
doi:10.1016/j.jpowsour.2011.11.034

VB2+/PC diffractometer, with a Cu-K_α operating at 200 mA and 40 kV and a scan rate of 10° min^{-1}. The samples were analyzed at big angle; the absorbance angle (2θ) was in the range of 10–90°. The sample morphology was examined by using a S4700s scanning electron microscope (FSEM, Hitachi, Japan).

2.3. Electrochemical experiments of $AgCuO_2$ electrode

800 mg $AgCuO_2$ powder and 200 mg expended graphite were adequately mixed in agate mortar for 20 min and three drops of 40% KOH were added to this mixture followed by stirring equably, then the product was rolled on a rolling machine to form $AgCuO_2$ foils with a thickness of 80 μm. The foils were then moved onto a foam nickel net (1 cm × 1 cm) current collector and pressed under 10 MPa to manufacture $AgCuO_2$ electrodes. A Zn(Hg)/ZnO electrode was employed as reference electrode, pure nickel wire as auxiliary electrode and 35% KOH solution as electrolyte. After aging for 12 h, the CV test and charge–discharge test were carried out by using a CS300 electrochemistry workstation and a LAND CT 2001A battery test system (Jinnuo Corp., China) respectively.

3. Results and discussion

Fig. 1 is the FSEM photographs of $AgCuO_2$ at different magnifications. It can be seen that the $AgCuO_2$ crystals present thorn-balls form of about 30 μm in diameter. It is clear that at high magnification, the $AgCuO_2$ thorn-ball is composed of many one-dimension linear crystals arranged in a certain sequence. Fig. 2 is the XRD pattern of $AgCuO_2$ sample. Compared with $AgCuO_2$ standard diffraction pattern, we can conclude that the sample is pure $AgCuO_2$ [13]. Based on Scatter formula and the XRD result, the calculated size of the $AgCuO_2$ sample is 26 nm. This result approximately conforms to the FSEM examination.

CV test was firstly carried out to explore the electrochemical property of $AgCuO_2$ electrode. Fig. 3 is the CV curve of $AgCuO_2$ sample at a scan speed of 1 mV s^{-1}. It can be seen that there occur 5 pairs of redox peaks, namely, A: 1.056 and 0.819 V, B: 1.285 and 1.107 V, C: 1.696 and 1.491 V, D: 1.961 and 1.647 V and E: 2.014 and 1.822 V. The two oxidation peaks at 2.014 V and 1.961 V almost overlap each other, meaning the potentials of the two electrode processes are very close. According to the existing references, the reduction of $AgCuO_2$ is involved in the reduction processes of Cu(III) and Ag(I), so there must be four corresponding independent redox electric pairs. However, 5 pairs appear as a matter of fact. There occur two questionable points: (1) the references [10] attribute the reduction peaks both at 1.491 V and the succeeding 1.647 V to the discharge process of Ag(I) at 1.647 V, but it is well known that usually Ag(I) in the electrode only has one reduction peak under the same test condition after the first discharge process of $AgCuO_2$ at 1.822 V. (2) It is deemed that trivalent Cu like $NaCuO_2$ is very unstable in alkaline aqueous solution, but in our experiment, $AgCuO_2$ can exist in alkaline solution for months without obvious decomposition. Therefore, it can be seen that $AgCuO_2$ is quite different from $NaCuO_2$ in structure and we believe that the above 5 pairs of redox peaks correspond to 5 independent reactions respectively: Pair A and B correspond to the redox reactions peaks of Cu(II) and Cu(I) species respectively. Pair C is attributed to the redox peak of Ag(I). In combination with the reference [6], we have noticed that pair E comes from the reaction of Ag(II). In this case, pair D must be the redox peak of Cu(III), not the peak of impurity Ag(I) which has been affirmed by the existing references [10].

In order to make a quantitative analysis on the base of mathematics and accordingly determine the above electrochemical processes and the electron transfer numbers of the redox processes for the 5 peak pairs more precisely, numerical integration of the

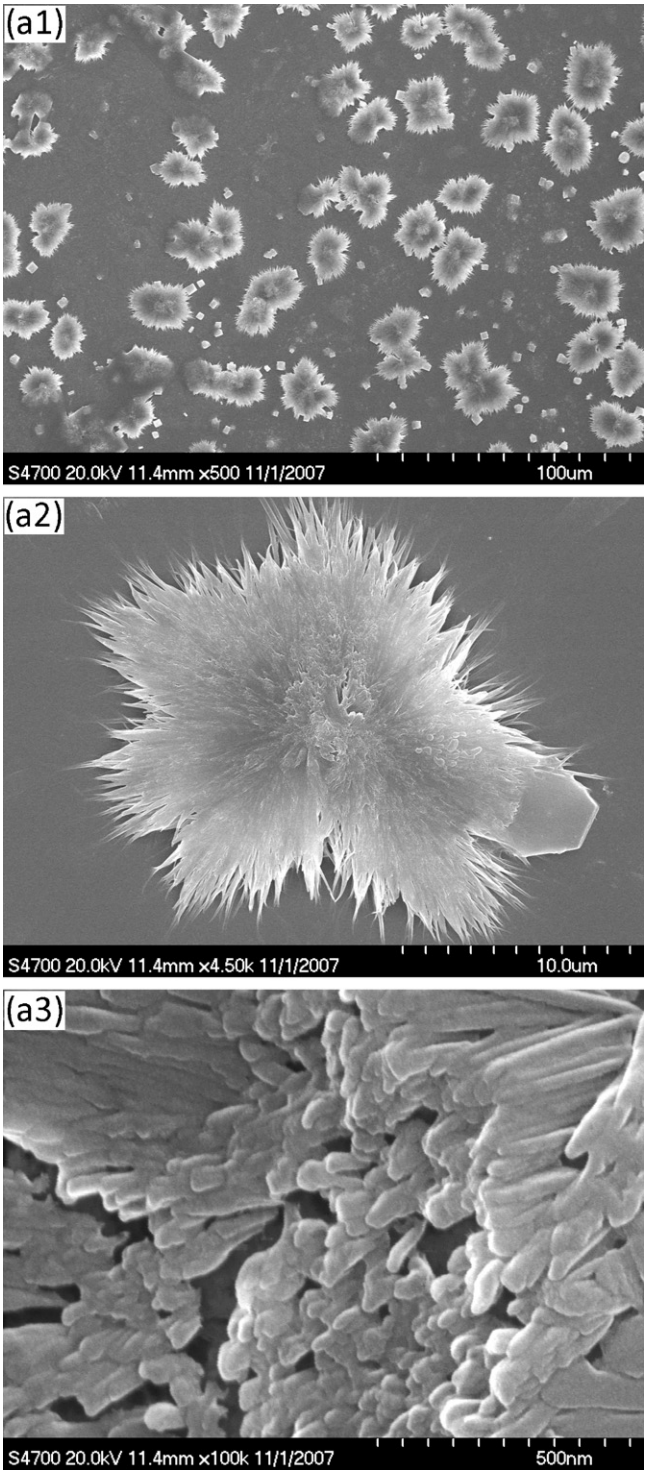

Fig. 1. The FSEM pictures of $AgCuO_2$.

CV curves for the third cycle was carried out and electric quantity analysis was performed. The results are sown in Table 1.

It can be seen that the charge capacity and discharge capacity are 25.953 C ($AgCuO_2$: 16.5 mg, 436.9 mAh) and 24.459 C (411.8 mAh), respectively. The efficiency of charge/discharge is 94.2%. According to Faraday Law and molecular weight of $AgCuO_2$, the theoretical electric quantity for 4 electron reduction for $AgCuO_2$ is 526.9 mAh, or 131.7 mAh for single electron reduction, meaning that $AgCuO_2$ offers 78.2% of theoretical capacity in the actual discharge process. The decrease in actual capacity possibly comes from the utilization

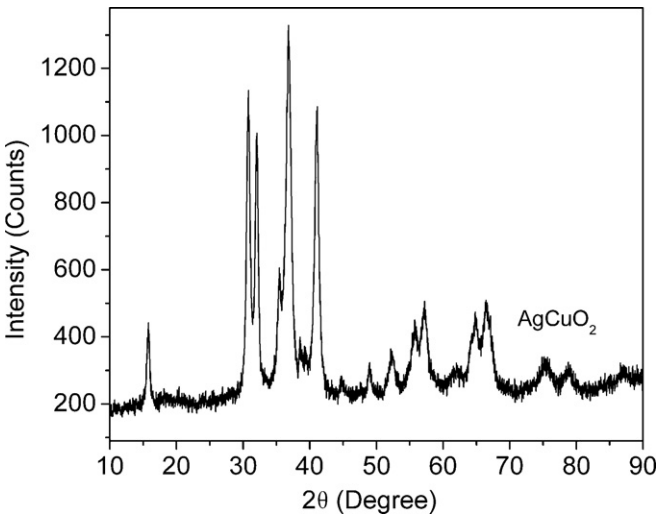

Fig. 2. The XRD pattern of as-prepared $AgCuO_2$.

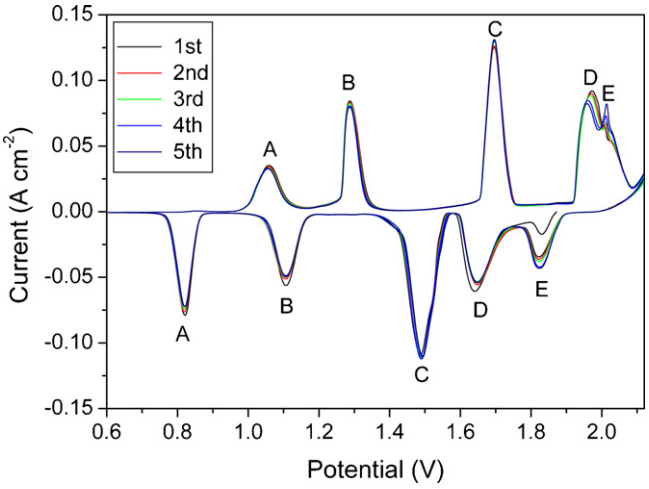

Fig. 3. The CV curves of $AgCuO_2$ electrode at a scan rate of 1 mV s^{-1} (vs. Zn(Hg)/ZnO).

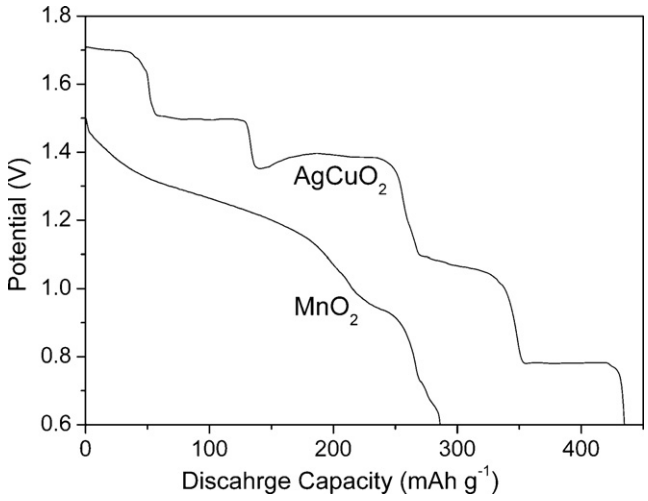

Fig. 4. The discharge curves of $AgCuO_2$ and MnO_2 electrode under 60 mA g^{-1}.

rate and electrochemical activity. It is easy to find through analyzing Table 1 that the total discharge capacity of D (86.2 mAh) and E (43.9 mAh) is 130.1 mAh, very close to 131.7 mAh of theoretical single electron capacity, meaning that the reduction for $AgCuO_2$ of high valence ion is the process which takes place in the manner of transferring 1/3 of the electron capacity for Ag(II) at 1.822 V followed by transferring 2/3 of the electron capacity for Cu(III) at 1.647 V, not simply transferring from Cu(III) to Cu(II). That is because Ag(I) can be oxidized into Ag(II) reversibly and Ag(I) and Cu(III) can partially transform into Ag(II) and Cu(II) respectively through their self-electron-deviation, thus decreasing the actual potential of Cu(III) compound, and considerably increasing the stability of $AgCuO_2$. To summarize the above discussion, it is more reasonable to regard $Ag(I)Cu(III)O_2$ as $Ag_2(I)\,Ag(II)Cu(II)Cu_2(III)O_6$. However, it is hard to carry out the similar electron transfer on Na(I) and Cu(III) for the existing $NaCuO_2$, thus leading to the bad storage property of $NaCuO_2$.

Similarly, at the succeeding potential (1.491 V) for pair C, the discharge capacity is 136.1 mAh, which might approximately be attributed to the single electron discharge capacity of Ag(I). At the lower potential of pair B and A, the discharge capacities are attributed to the processes of Cu(II) → Cu(I) and Cu(I) → Cu(0), respectively. However, they are only 72.9 mAh and 72.6 mAh respectively, showing that Cu(II) and Cu(I) of low valence ions only have a utilization rate as low as 55.4% in addition to low potential. The future study should be focused on changing grain size and creating micro-nano structure to increase the utilization rate of the active material.

In the initial oxidation period of $AgCuO_2$, there are only Ag(0) and Cu(0) in the electrode. With increasing reaction time, Cu(I) is earlier formed on partial surface of Cu particles and resistant to the contact between conductive agent and Cu(0) inside Cu particle, leading to the fast oxidation of the new formed Cu(I) into Cu(II), meanwhile, the resultant Cu(II) is able to oxidize the Cu(0) inside particles into Cu(I) coupled with the reduction of Cu(II) itself into Cu(I) gradually through redox process. This process is embodied in the result that the electric quantity of Cu(0) → Cu(I) is far less than that of Cu(I) → Cu(II). The similar phenomenon also happens to the succeeding processes of Ag(0) → Ag(I) and Ag(I) → Ag(II).

In order to fully reflect the discharge capacity of $AgCuO_2$ in maximum extent, galvanostatic discharge tests of $AgCuO_2$ and MnO_2 electrodes were performed at low current density. Fig. 4 shows that $AgCuO_2$ offers 434.2 mAh g^{-1}, but still lower than its theoretical capacity of 527 mAh g^{-1}, meaning that the inner active material is not fully involved in the electrode reaction. However, the capacity of 434.2 mAh g^{-1} for $AgCuO_2$ is far higher than that of 285.5 mAh g^{-1} for MnO_2, which benefits from the multi-electron reduction of $AgCuO_2$ itself. As for the super high discharge plateau, it is quite suitable to becoming a new generation of positive electrode material of alkaline batteries.

It can be seen that there occur 5 discharge plateaus at 1.67 V, 1.52 V, 1.41 V, 1.07 V and 0.79 V during discharge process.

Table 1
Electric quantity analysis of $AgCuO_2$ electrode by the CV results in Fig. 3.

Electric pair	A		B		C		D		E	
	C	mAh	C	mAh	C	mAh	C	mAh	C	mAh
Reduction electric quantity	4.329	72.9	4.313	72.6	8.085	136.1	5.123	86.2	2.609	43.9
Oxidation electric quantity	2.826	47.6	4.801	80.8	7.508	126.4	10.818	182.1		

The corresponding capacities are 49.2 mAh g^{-1}, 86.8 mAh g^{-1}, 132.6 mAh g^{-1}, 83.2 mAh g^{-1} and 82.4 mAh g^{-1}, respectively. In combination with the analysis of the CV test, we believe that these discharge plateaus correspond to Ag(II) of 1/3 electron, Cu(III) of 2/3 electron, Ag(I) of 1electron, Cu(II) of 0.63 electron and Cu(I) of 0.63 electron, respectively. It can be seen that the decrease in actual discharge capacity mainly comes from the low activity of Cu(II) and Cu(I) which are the resultants of $AgCuO_2$ reduction and the low utilization rate. To combine the analysis of CV data, we conclude that the following reactions are involved in the discharge of $Ag_2(I)Ag(II)Cu(II)Cu_2(III)O_6$:

$$2Ag_2(I)Ag(II)Cu(II)Cu_2(III)O_6 + H_2O + 2e \rightarrow 2Ag_3(I)Cu(II)Cu_2(III)O_{5.5} + 2OH^- \quad (1)$$

$$2Ag_3(I)Cu(II)Cu_2(III)O_{5.5} + 2H_2O + 4e \rightarrow 2Ag_3(I)Cu_3(II)O_{4.5} + 4OH^- \quad (2)$$

$$2Ag_3(I)Cu_3(II)O_{4.5} + 3H_2O + 6e \rightarrow 2Ag_3(0)Cu_3(II)O_3 + 6OH^- (1.41\,V) \quad (3)$$

$$2Ag_3(0)Cu_3(II)O_3 + 3H_2O + 6e \rightarrow 2Ag_3(0)Cu_3(I)O_{1.5} + 6OH^- (1.07\,V) \quad (4)$$

$$2Ag_3(0)Cu_3(I)O_{1.5} + 3H_2O + 6e \rightarrow 2Ag_3(0)Cu_3(0) + 6OH^- (0.79\,V) \quad (5)$$

$$\text{Total}: 2Ag_2(I)Ag(II)Cu(II)Cu_2(III)O_6 + 12H_2O + 24e \rightarrow 2Ag_3(0)Cu_3(0) + 24OH^- \quad (6)$$

It can be seen in Fig. 4 that in the initial discharge period of Ag(II) of 1/3 electron and Cu(III) of 2/3 electron, the discharge curve presents flat, their discharge products are Ag(I) and Cu(II), respectively. In the succeeding period of Ag(I) → Ag(0), the increase in discharge voltage is observed because Ag of good conductance is formed, leading to the increase in electrode conductance. In the low voltage stage of Cu(II) → Cu(I), with consumption of Cu(II), the polarization is gradually increased, thus causing slight decrease in discharge voltage. During the final period of Cu(I) → Cu(0), slight increase in voltage is presented because Cu is formed, also leading to improvement of conductivity.

In order to fully verify the redox mechanism of the $AgCuO_2$, the XRD analysis results for the charged $AgCuO_2$ electrode after each reduction step at 60 mA g^{-1} are shown in Fig. 5. It can be seen that the diffraction peak at 26.54° of carbon appears for all curves. That results from the graphite addition for increasing the conductivity of the $AgCuO_2$ electrode. Curve (a) is the XRD pattern of the fully charged $AgCuO_2$ electrode. The diffraction peaks appear at 30.91°, 32.10°, 37.01°, 37.15° and 44.12° in respect to (2 0 0), (0 0 2), (−1 1 1), (−2 0 2) and (1 1 1) crystal lines of $AgCuO_2$ (PDF# 01-070-8903), which indicates that the charged product is $AgCuO_2$.

Curve (b) shows the X-ray diffraction pattern for $AgCuO_2$ after the first discharging platform (1.67 V). It can be seen that a little amount of Ag $(I)_2O$, which may comes from the reduction of Ag(II), is generated in the sample. That indicates a part of Ag in $AgCuO_2$ has expressed the characteristics of Ag(II). In addition, it is also observed that the diffraction peaks at 33.50°, 34.77°

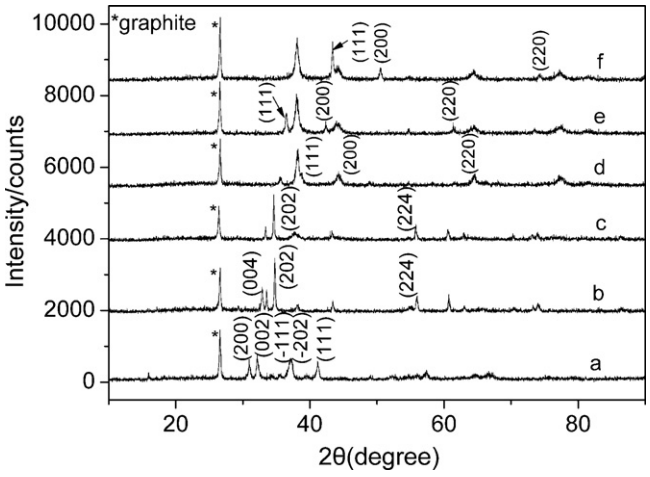

Fig. 5. The XRD patterns for the charged $AgCuO_2$ electrode after each reduction step at low current density of 60 mA g^{-1}. (a) Fully charged $AgCuO_2$ electrode; (b) the reduction product after discharging at 1.67 V; (c) the product after discharging at 1.52 V; (d) after discharging at 1.41 V; (e) after discharging at 1.07 V; (f) after discharging at 0.79 V).

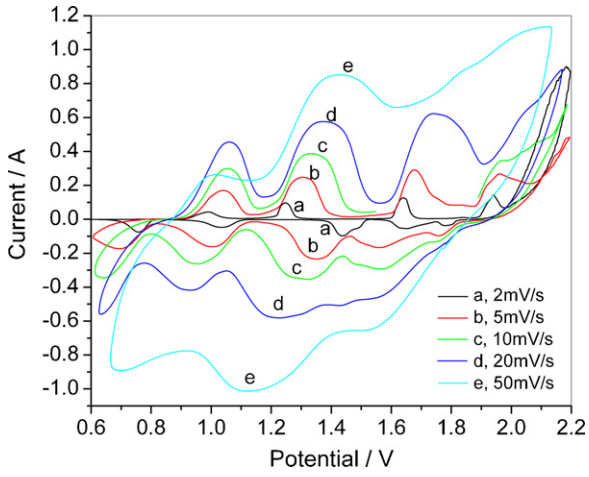

Fig. 6. The CV curves of $AgCuO_2$ electrode at different scan rate.

and 55.90° correspond to (0 0 4), (2 0 2) and (2 2 4) crystal lines of $Ag_2Cu_2O_3$ (PDF#01-073-6753) respectively, indicating that a part of the Cu(III) in $AgCuO_2$ is reduced to Cu(II). That demonstrates the reduction process of $AgCuO_2$ is a mixed process. Curve (c) is the XRD pattern for $AgCuO_2$ after the second discharge platform (1.52 V). It

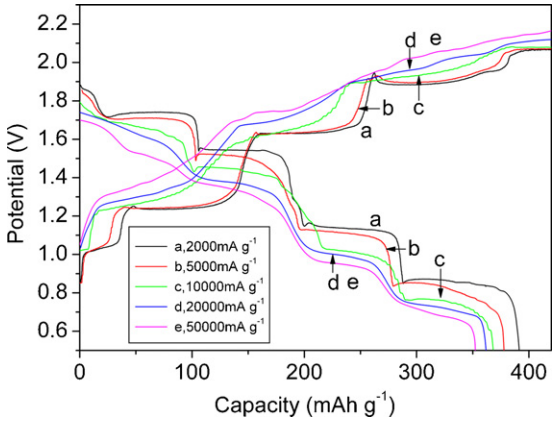

Fig. 7. The charge/discharge property of $AgCuO_2$ electrodes.

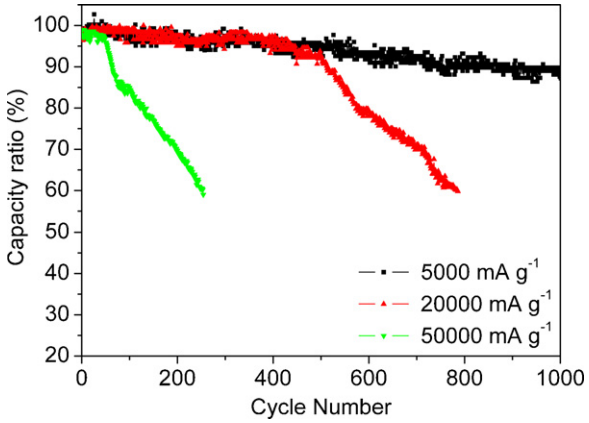

Fig. 8. The cycle property of $AgCuO_2$ electrodes under different charge/discharge speed.

is observed that the main reduction product is $Ag_2Cu_2O_3$, which indicates the $AgCuO_2$ electrode continues to form $Ag_2Cu_2O_3$ on the discharge platform of 1.52 V. Curve (d) shows the X-ray diffraction pattern for $AgCuO_2$ after the third discharge platform (1.41 V). The diffraction peaks appear at 38.12°, 44.28° and 64.45°, corresponding to (1 1 1), (2 0 0) and (2 2 0) crystal lines of Ag(0) respectively. And the peaks at 35.54° and 38.75° correspond to Cu(II)O. Thus it is concluded that the corresponding reduction product is Ag(0) and Cu(II) at this stage. Curve (e) is the XRD pattern for the $AgCuO_2$ electrode after the fourth discharge platform (1.07 V). Compared with curve (d), the new diffraction peaks appear at 36.42°, 42.31° and 61.38°, corresponding to the (1 1 1), (2 0 0) and (2 2 0) crystal lines of Cu_2O respectively. So the electrochemical reaction on the platform may be involved in $Ag(0) + Cu(II)O \rightarrow Ag(0) + Cu(I)_2O$. Curve (f) is the XRD pattern for the $AgCuO_2$ electrode after the fifth discharge platform (0.79 V). It can be seen that the new diffraction peaks at 43.34°, 50.48° and 74.17° correspond to the (1 1 1), (2 0 0) and (2 2 0) crystal lines of Cu(0) respectively. Thus the electrochemical reaction at this stage is involved in $Ag(0) + Cu(I)_2O \rightarrow Ag(0) + Cu(0)$.

Fig. 6 demonstrates CV curves of $AgCuO_2$ at various scan rates. With increasing scan rate from 2 mV s^{-1} to 50 mV s^{-1}, oxidation peak of $AgCuO_2$ increases. It is found that when scan rate reaches 50 mV s^{-1}, the anodic scan is shortened to 32 s, the charge process is finished in such a short time and a capacity of 337.2 mAh g^{-1} is offered, showing excellent charge/discharge ability in extra short time. Therefore, a galvanical charge/discharge curve was measured at 2000–50,000 mA g^{-1} at super high speed. The result is shown in Fig. 7. It can be seen that with increasing charge/discharge current, the charge/discharge plateau of $AgCuO_2$ still presents flat and keeps relatively stable although cycling capacity slightly decays from 391 mAh g^{-1}(2000 mA g^{-1}) to 352 mAh g^{-1}(50,000 mA g^{-1}). Obviously, the waiting time is considerably shortened, from 12.6 min at 2000 mA g^{-1} to 29 s at 50,000 mA g^{-1}. We think that the super high speed ability benefits from the diplex ability of transfer electron on the one hand and from its open structure form of layered and nano linear structure on the other hand, which favors the fast exchange and transfer of electrons and ions in charge/discharge process.

We have noticed that although $AgCuO_2$ has good electrochemical property and charge/discharge ability at 50,000 mA g^{-1}, the electrode still undergoes polarization. The polarization and high current (9.55 mg at 477.5 mA) generate obvious heat, thus shortening its cycle life. So cycle life was also measured at 5000–50,000 mA g^{-1}. As can be seen in Fig. 8, $AgCuO_2$ electrode retains 87% cycling capacity at 5000 mA g^{-1} after 1000 cycles. When the current density increases from 20,000 mA g^{-1} to 50,000 mA g^{-1}, the cycle life deceases from 786 to 253 cycles, respectively. We found that the electrolyte temperature rose from 30 °C to 52 °C in the process of charge and discharge, and large amount of oxygen was generated on the positive electrode at the late charging stage simultaneously. The joule heat generated by large current and oxygen releasing caused the volatilization of water in KOH electrolyte and then led to partial drought of the electrode, inhibiting the active substances of this part of electrode from full participation in the electrode reaction, thus decreasing the charge–discharge capacity. The latest mathematic model shows that the life span of the electrode is able to be shortened from the existing 29 s down to 7.3 s, meaning that the charge process of power batteries made of $AgCuO_2$ can be completed instantaneously.

4. Conclusions

It is demonstrated that $AgCuO_2$ presents thorn-ball form composed of one-dimension nano-meter linear crystals. CV tests indicate that the charge/discharge process of $AgCuO_2$ is not the single electron transfer for Cu(III) but the fast dual electron transfer for Ag(II) and Cu(III). The super high speed ability of charge/discharge makes the charge or discharge time of the $AgCuO_2$ electrode shorter than 29 s, which will make it possible to replenish energy as fast as refilling fuel vehicles in the future.

Acknowledgements

This work was supported by Beijing Nova Program (2008B17), the Foundation of Excellent Doctoral Dissertation of Beijing City (YB20081001002) and National Natural Science Foundation of China (21006003). The authors thank Prof. Xiaoguang Liu for the important discussions and modification of the manuscript.

References

[1] B. Kang, Y.S. Meng, J. Breĭger, C.P. Grey, G. Ceder, Science 311 (2006) 977.
[2] A. Kuwahara, S.##1 Suzuki, M. Miyayama, Ceram. Int. 34 (2008) 863.
[3] X.L. Wu, L.Y. Jiang, F.F. Cao, Y.G. Guo, L.J. Wan, Adv. Mater. 21 (2009) 2710.
[4] B. Kang, G. Ceder, Nature 458 (2009) 190.
[5] M. Holzapfel, H. Buqa, W. Scheifele, P. Nova'ka, F.M. Petrat, Chem. Commun. (2005) 1566.
[6] J. Pan, Y. Sun, Z. Wang, P. Wan, X. Liu, M. Fan, J. Mater. Chem. 17 (2007) 4820.
[7] P. Gómez-Romero, E.M. Tejada-Rosales, M.R. Palacín, Angew. Chem. Int. Ed. 38 (1999) 524.
[8] C.D. May, J.T. Vaughey, Electrochem. Commun. 6 (2004) 1075.
[9] D. Muñoz-Rojas, G. Subías, J. Fraxedas, P. Gómez-Romero, N. Casañ-Pastor, J. Phys. Chem. B 109 (2005) 6193.
[10] F. Wang, C. Eylem, K. Nanjundaswamy, N. Iltchev, Electrochem. Solid-State Lett. 7 (2004) A346.
[11] T.W. Jones, J.S. Forrester, A. Hamilton, M.G. Rose, S.W. Donne, J. Power Sources 172 (2007) 962.
[12] T. Zhang, X. Zhang, F.Hu. Chin, J. Inorg. Chem. 21 (2005) 1077.
[13] J. Curda, W. Klein, M. Jansen, J. Solid-State Chem. 162 (2001) 220.